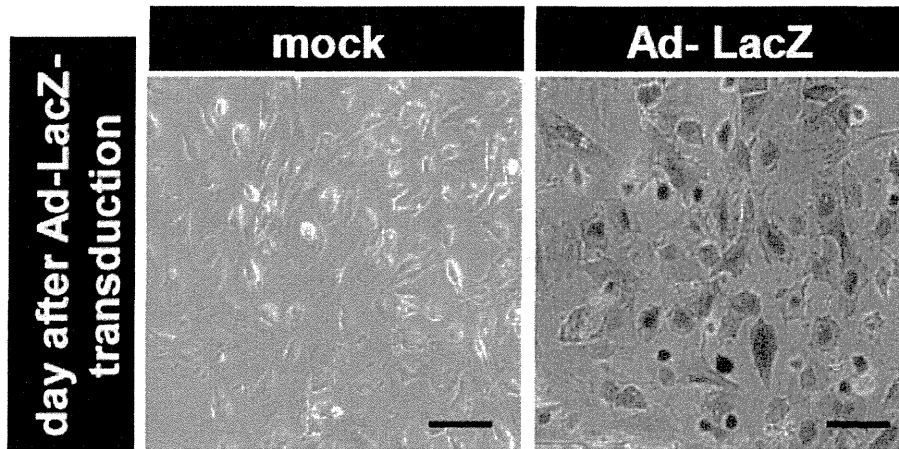


**Fig. S2** *c/EBPα*, *c/EBPβ*, or *TGFBR2* were knocked-down in the HBCs by *si-c/EBPα*, *si-c/EBPβ*, or *si-TGFBR2* transfection, respectively.

The HBCs were transfected with 50 nM of *si-control*, *si-c/EBPα*, *si-c/EBPβ*, or *si-TGFBR2*. Two days after transfection, the gene expression levels of *c/EBPα*, *c/EBPβ*, or *TGFBR2* were examined by real-time RT-PCR in *si-c/EBPα*-, *si-c/EBPβ*-, or *si-TGFBR2*-transfected cells, respectively. On the y axis, the gene expression levels of *c/EBPα*, *c/EBPβ*, or *TGFBR2* in *si-control*-transfected cells were taken as 1.0. \*\* $P < 0.01$  (compared with the *si-control*-transfected cells).



**Fig. S3 Ad vectors efficiently transduced the HBCs.**

The HBCs were transduced with 3,000 VP/cell of Ad-LacZ for 1.5 hr. The day after transduction, X-gal staining was performed. The scale bars represent 50  $\mu$ m.

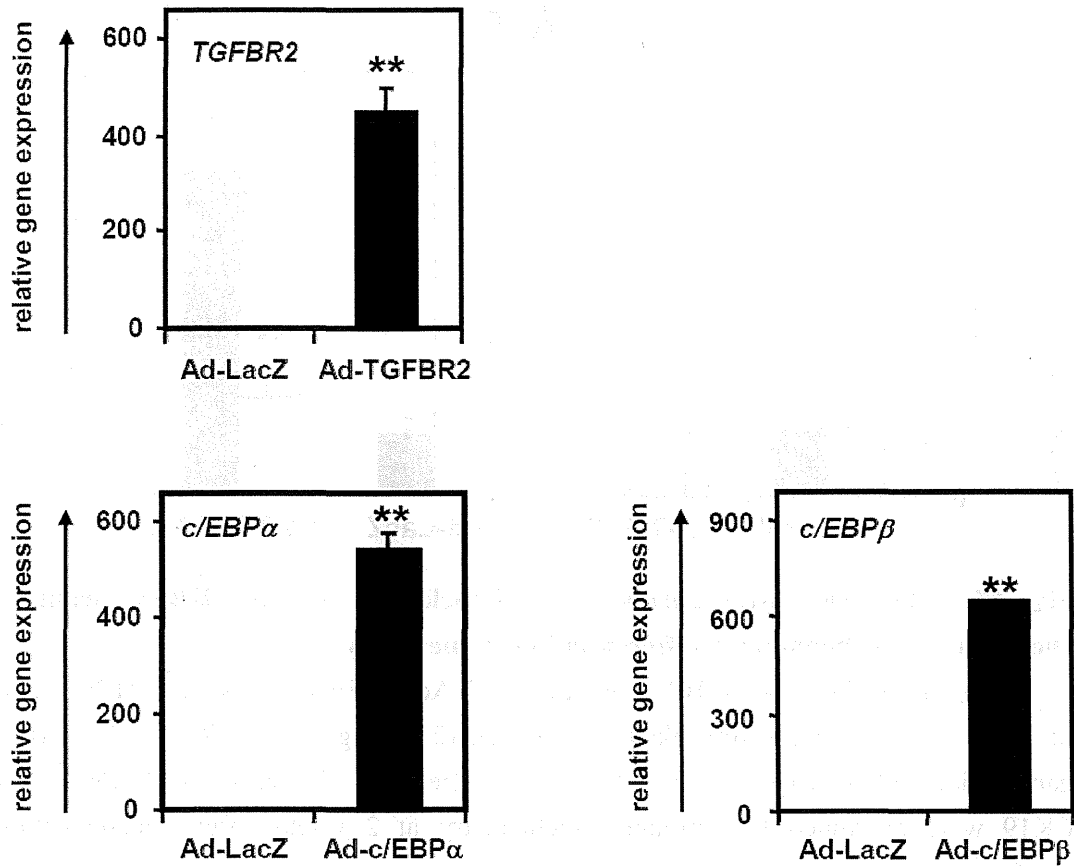


**Fig. S4** *c/EBP $\alpha$* , *c/EBP $\beta$* , or *TGFBR2* were overexpressed in the HBCs by Ad-*c/EBP $\alpha$* , Ad-*c/EBP $\beta$* , or Ad-*TGFBR2* transduction, respectively.

The HBCs were transduced with 3,000 VP/cells of Ad-*c/EBP $\alpha$* , Ad-*c/EBP $\beta$* , or Ad-*TGFBR2* for 1.5 hr. Two days after Ad vectors transduction, the gene expression levels of *c/EBP $\alpha$* , *c/EBP $\beta$* , or *TGFBR2* were examined by real-time RT-PCR in Ad-*c/EBP $\alpha$* -, Ad-*c/EBP $\beta$* -, or Ad-*TGFBR2*-transduced cells, respectively. On the y axis, the gene expression levels of *c/EBP $\alpha$* , *c/EBP $\beta$* , or *TGFBR2* in Ad-*LacZ*-transduced cells were taken as 1.0. \*\* $P < 0.01$  (compared with the Ad-*LacZ*-transfected cells).

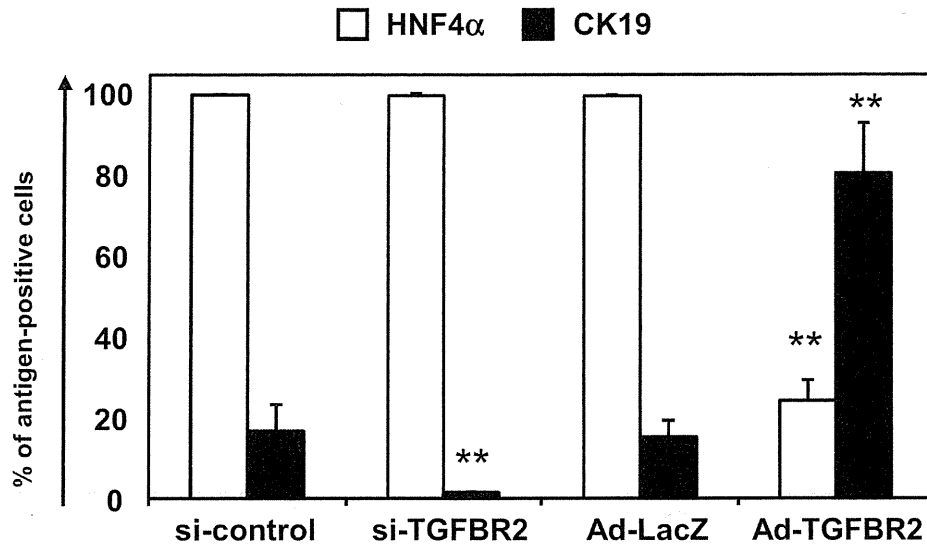


**Fig. S5 TGFBR2 overexpression or knockdown in the HBCs promotes cholangiocyte or hepatocyte differentiation, respectively.**

The si-control-, si-TGFBR2-, Ad-LacZ- or Ad-TGFBR2-transduced HBCs (total of  $1.0 \times 10^6$  cells) were transplanted into  $\text{CCl}_4$  (2 mL/kg)-treated Rag2/IL2 receptor gamma double knockout mice by intrasplenic injection. Expressions of HNF4 $\alpha$  and CK19 were examined by immunohistochemistry at 2 weeks after transplantation. Semiquantitative analysis of the immunofluorescent staining was performed in the human cell clusters. \* $P < 0.05$ ; \*\* $P < 0.01$ .

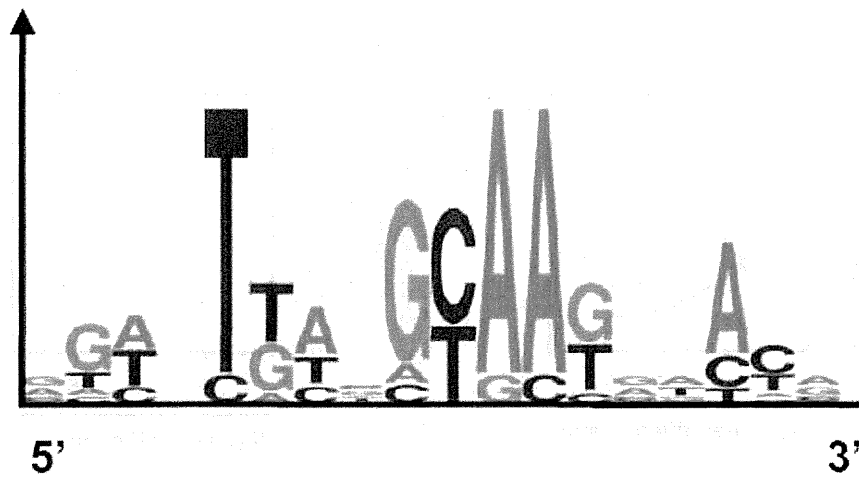


**Fig. S6 c/EBP-binding site on the TGFBR2 promoter region**

The consensus sequence of the c/EBP-binding site is described.  
 (<http://www.cbil.upenn.edu/cgi-bin/tess/tess>).

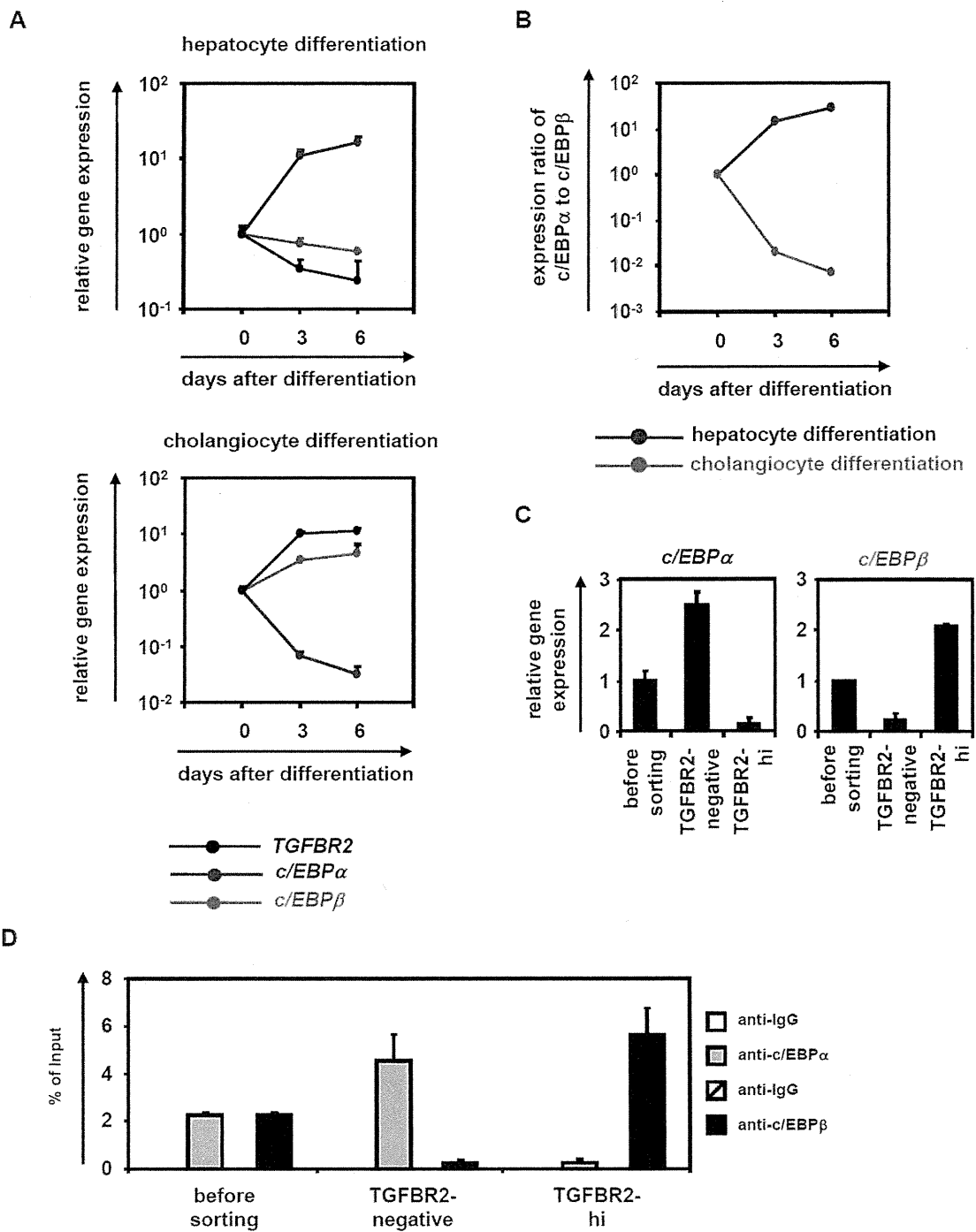


**Fig. S7** Temporal gene expression levels of *TGFBR2*, *c/EBPα*, and *c/EBPβ* in hepatocyte and cholangiocyte differentiation.

The HBCs were differentiated into hepatocyte-like cells or cholangiocyte-like cells as shown in figure 1A. (A) Temporal gene expression levels of *TGFBR2*,

*c/EBPα*, and *c/EBPβ* in hepatocyte differentiation and cholangiocyte differentiation of the HBCs were examined by real-time RT-PCR. On the y axis, the gene expression levels in the HBCs were taken as 1.0. **(B)** The temporal ratio of *c/EBPα* to *c/EBPβ* was demonstrated in hepatocyte and cholangiocyte differentiation. The ratio of *c/EBPα* to *c/EBPβ* in the HBCs was taken as 1.0. **(C)** The HBCs were cultured on Matrigel for 5 days, and then the expression level of TGFBR2 was examined by FACS analysis. TGFBR2-negative, -lo, and -hi populations were collected as described in figure 1F. Real-time RT-PCR analysis was performed in three populations (before sorting, TGFBR-negative, and TGFBR2-hi) to measure the expression levels of *c/EBPα* and *c/EBPβ*. **(D)** The recruitment of *c/EBPα* or *c/EBPβ* to the TGFBR2 promoter region in three populations (before sorting, TGFBR-negative, and TGFBR2-hi) was examined by ChIP assay.

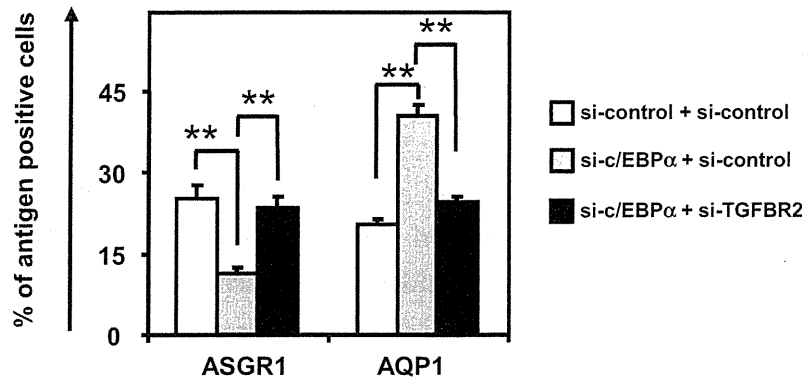


**Fig. S8 Inhibition of hepatocyte differentiation by si-c/EBP $\alpha$  transfection was rescued by si-TGFBR2 transfection.**

The HBCs were transfected with 50 nM of each of si-control + si-control, si-c/EBP $\alpha$  + si-control, or si-c/EBP $\alpha$  + si-TGFBR2 and cultured with the differentiation hESF-DIF medium for 10 days. The efficiency of hepatocyte or cholangiocyte differentiation was measured by estimating the percentage of ASGR1- or AQP1-positive cells, respectively, using FACS analysis. \* $P$ <0.05; \*\* $P$ <0.01.



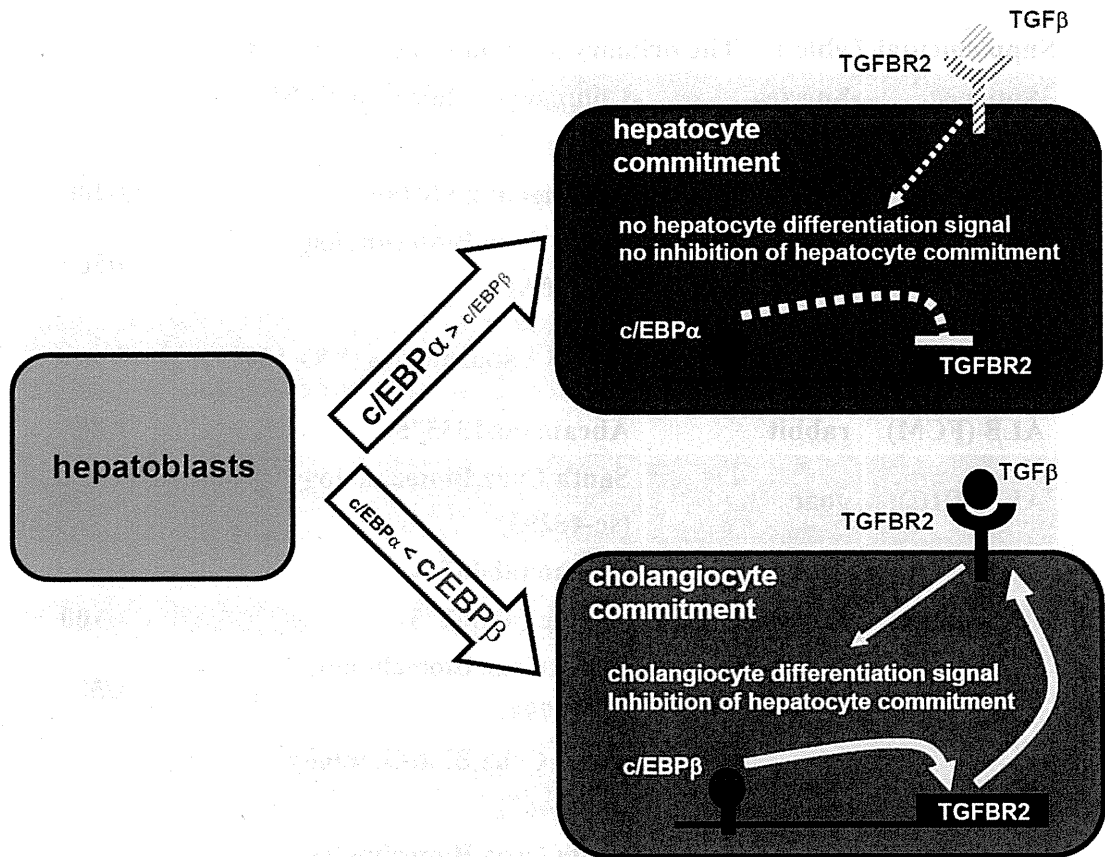


**Fig. S9** The lineage segregation of hepatoblasts might be explained by c/EBP-mediated control of TGFBR2 expression.

In hepatocyte differentiation from hepatoblasts, c/EBP $\alpha$  promotes hepatocyte differentiation via negative regulation of TGFBR2 expression. On the other hand, c/EBP $\beta$  promotes cholangiocyte differentiation via positive regulation of TGFBR2 expression in cholangiocyte differentiation.

**Supplemental Table 1 The primary antibodies used in this study**

<b>Antigen</b>	<b>Species</b>	<b>Company (catalog number)</b>	<b>Dilution</b>
<b>CK19</b>	<b>rabbit</b>	<b>Abcam (ab52625)</b>	<b>1/250</b>
<b>AFP</b>	<b>mouse</b>	<b>Cell Signaling (#3903)</b>	<b>1/100</b>
<b>c/EBP<math>\beta</math></b>	<b>rabbit</b>	<b>Santa Cruz Biotechnology (sc-150AC)</b>	<b>1/50</b>
<b>ALB (ELISA)</b>	<b>goat</b>	<b>Bethyl Laboratories (E80-129)</b>	
<b>ALB (FCM)</b>	<b>rabbit</b>	<b>Abcam (ab135575)</b>	<b>1/40</b>
<b>ALB (IHC)</b>	<b>goat</b>	<b>Santa Cruz Biotechnology (sc-46293)</b>	<b>1/200</b>
<b>c/EBP<math>\alpha</math></b>	<b>rabbit</b>	<b>Abcam (ab40764)</b>	<b>1/50</b>
<b>HNF4<math>\alpha</math></b>	<b>abcm</b>	<b>Abcam (ab36175)</b>	<b>1/100</b>
<b>TGFBR2</b>	<b>mouse</b>	<b>Santa Cruz Biotechnology (sc-17799)</b>	<b>1/50</b>
<b>ASGR1</b>	<b>goat</b>	<b>Santa Cruz Biotechnology (sc-13467)</b>	<b>1/50</b>
<b>CYP3A4</b>	<b>goat</b>	<b>Santa Cruz Biotechnology (sc-27639)</b>	<b>1/200</b>
<b>AQP1</b>	<b>mouse</b>	<b>Abcam (ab9566)</b>	<b>1/40</b>
<b>EpCAM</b>	<b>mouse</b>	<b>Miltenyi Biotec (130-091-254)</b>	<b>1/50</b>

**Supplemental Table 2 The secondary antibodies used in this study**

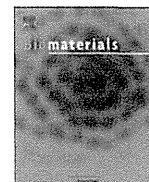
<b>Antigen</b>	<b>label</b>	<b>Company</b>	<b>Species</b>	<b>Dilution</b>
<b>rabbit IgG</b>	<b>alexa fluor 488</b>	<b>Molecular Probes</b>	<b>goat</b>	<b>1/1000</b>
<b>rabbit IgG</b>	<b>alexa fluor 488</b>	<b>Molecular Probes</b>	<b>chicken</b>	<b>1/1000</b>
<b>mouse IgG</b>	<b>alexa fluor 488</b>	<b>Molecular Probes</b>	<b>rabbit</b>	<b>1/1000</b>
<b>goat IgG</b>	<b>alexa fluor 488</b>	<b>Molecular Probes</b>	<b>rabbit</b>	<b>1/1000</b>
<b>rabbit IgG</b>	<b>alexa fluor 594</b>	<b>Molecular Probes</b>	<b>mouse</b>	<b>1/1000</b>
<b>goat IgG</b>	<b>alexa fluor 594</b>	<b>Molecular Probes</b>	<b>mouse</b>	<b>1/1000</b>
<b>goat IgG</b>	<b>alexa fluor 594</b>	<b>Molecular Probes</b>	<b>chicken</b>	<b>1/1000</b>
<b>goat IgG</b>	<b>alexa fluor 594</b>	<b>Molecular Probes</b>	<b>donkey</b>	<b>1/1000</b>
<b>mouse IgG</b>	<b>alexa fluor 594</b>	<b>Molecular Probes</b>	<b>chicken</b>	<b>1/1000</b>

**Supplemental Table 3 The primers used for real-time RT-PCR in this study**

Genes	Primers (forward/reverse; 5' to 3')
CK7	AGACGGAGTTGACAGAGCTG/GGATGGCCCGGTTTCATCTC
CK19	CTCCCGCGACTACAGCCACT/TCAGCTCATCCAGCACCCCTG
HES1	ATGGAGAAAAATTCCTCGTCCC/TTCAGAGCATCCAAAATCAGTGT
SOX9	TTTCCAAGACACAAAACATGA/AAAGTCCAGTTTCTCGTTGA
integrin $\beta$ 4	GCAGCTTCCAAATCACAGAGG/CCAGATCATCGGACATGGAGTT
TO	GGCAGCGAAGAAGACAAATC/TCGAACAGAATCCAACCTCC
$\alpha$ AT	ACTGTCAACTTCGGGGACAC/CATGCCTAAACGCTTCATCA
ALB	GCACAGAATCCTTGGTGAACAG/ATGGAAGGTGAATGTTTTAGCA
TGFBR2	GGAAACTTGACTGCACCGTT/CTGCACATCGTCTCTGTTG
c/EBP $\alpha$	TTCACATTGCACAAGGCACT/GAGGGACCGGAGTTATGACA
c/EBP $\beta$	CGTGTACACACGCGTTCAG/CTCTCTGCTTCTCCCTCTGC
HNF6	CAAAACCCTGGAGCAAACCTCAA/TGTGTTGCCTCTATCCTTCCC
HNF1 $\beta$	ACCAAGCCGGTCTTCCATACT/GGTGTGTCATAGTCGTCGCC
CYP2D6	CTTTCGCCCAACGGTCTC/TTTTGGAAGCGTAGGACCTTG
TTR	TCATCGTCTGCTCCTCCTCT/AGGTGTCATCAGCAGCCTTT
HNF1 $\alpha$	AACACCTCAACAAGGGCACTC/CCCCACTTGAACGGTTCCT
CYP3A4	AAGTCGCCTCGAAGATACACA/AAGGAGAGAACACTGCTCGTG
mouse $\alpha$ AT	TTGCTCGACACAACATGGAAT/ACGTCCCAGTTTGACATCTCT
mouse CYP7A1	GCTGTGGTAGTGAGCTGTTG/GTTGTCCAAAGGAGGTTACCC
mouse AQP1	AGGCTTCAATTACCCACTGG/CTTTGGGCCAGAGTAGCGAT
mouse integrin $\beta$ 4	AGAGCTGTACCGAGTGCATC/TGGTGTGATCTGGGTGTTCT

**Supplemental Table 4 The primers used for ChIP assay in this study**

	Primers (forward/reverse; 5' to 3')
c/EBP binding site A	TCACAAC TTTCTAAGTCCCAATTT/ACTGAGGCAGGGACTGTGTC
c/EBP binding site B	AACTGAAATGTCTTCCTTTTCAA/CAGGAGGAGTAGAGCCAGCA
c/EBP binding site C	GCCACATTGTGTTTTAGGA/TTAGCCGAGAATGATGTCACC
c/EBP binding site D	CCAGAGGGCTGTACAGAATCA/CCAGATTTGCCCAAGACATT
c/EBP binding site E	TGCCTACTGGGTGCTAGAGG/AACCTTCAGAGACAGCGATCA
$\beta$ -actin	CCGGCGGGTCTTTGTCTGAGC/GGGCCGGCCGCGTTATTACCA



## 3D spheroid culture of hESC/hiPSC-derived hepatocyte-like cells for drug toxicity testing

Kazuo Takayama<sup>a,b</sup>, Kenji Kawabata<sup>b,c</sup>, Yasuhito Nagamoto<sup>a,b</sup>, Keisuke Kishimoto<sup>a,b</sup>, Katsuhisa Tashiro<sup>b</sup>, Fuminori Sakurai<sup>a</sup>, Masashi Tachibana<sup>a</sup>, Katsuhiko Kanda<sup>d</sup>, Takao Hayakawa<sup>e</sup>, Miho Kusuda Furue<sup>f,g</sup>, Hiroyuki Mizuguchi<sup>a,b,h,\*</sup>

<sup>a</sup> Laboratory of Biochemistry and Molecular Biology, Graduate School of Pharmaceutical Sciences, Osaka University, Osaka 565-0871, Japan

<sup>b</sup> Laboratory of Stem Cell Regulation, National Institute of Biomedical Innovation, Osaka 567-0085, Japan

<sup>c</sup> Laboratory of Biomedical Innovation, Graduate School of Pharmaceutical Sciences, Osaka University, Osaka 565-0871, Japan

<sup>d</sup> Pharma Business Project, Corporate Projects Center, Corporate Strategy Division, Hitachi High-Technologies Corporation, Ibaraki 312-8504, Japan

<sup>e</sup> Pharmaceutical Research and Technology Institute, Kinki University, Osaka 577-8502, Japan

<sup>f</sup> Laboratory of Embryonic Stem Cell Cultures, Department of Disease Bioresources Research, National Institute of Biomedical Innovation, Osaka 567-0085, Japan

<sup>g</sup> Department of Embryonic Stem Cell Research, Field of Stem Cell Research, Institute for Frontier Medical Sciences, Kyoto University, Kyoto 606-8507, Japan

<sup>h</sup> The Center for Advanced Medical Engineering and Informatics, Osaka University, Osaka 565-0871, Japan

### ARTICLE INFO

#### Article history:

Received 11 September 2012

Accepted 20 November 2012

Available online 8 December 2012

#### Keywords:

Hepatocyte-like cell

Human ES cell

Human iPS cell

Nanopillar plate

Drug screening

### ABSTRACT

Although it is expected that hepatocyte-like cells differentiated from human embryonic stem (ES) cells or induced pluripotent stem (iPS) cells will be utilized in drug toxicity testing, the actual applicability of hepatocyte-like cells in this context has not been well examined so far. To generate mature hepatocyte-like cells that would be applicable for drug toxicity testing, we established a hepatocyte differentiation method that employs not only stage-specific transient overexpression of hepatocyte-related transcription factors but also a three-dimensional spheroid culture system using a Nanopillar Plate. We succeeded in establishing protocol that could generate more matured hepatocyte-like cells than our previous protocol. In addition, our hepatocyte-like cells could sensitively predict drug-induced hepatotoxicity, including reactive metabolite-mediated toxicity. In conclusion, our hepatocyte-like cells differentiated from human ES cells or iPS cells have potential to be applied in drug toxicity testing.

© 2012 Elsevier Ltd. All rights reserved.

### 1. Introduction

Hepatocyte-like cells that are generated from human embryonic stem cells (hESCs) [1] or human induced pluripotent stem cells (hiPSCs) [2] are expected to be used in drug screening instead of primary (or cryopreserved) human hepatocytes (PHs). We recently demonstrated that stage-specific transient transduction of transcription factors, in addition to treatment with optimal growth factors and cytokines, is useful for promoting hepatic differentiation [3–6]. The hepatocyte-like cells, which have many hepatocyte characteristics (the abilities to uptake low-density lipoprotein and Indocyanine green, store glycogen, and synthesize urea) and drug metabolism capacity, were generated from hESCs/hiPSCs by

combinational transduction of FOXA2 and HNF1 $\alpha$  [6]. However, further maturation of the hepatocyte-like cells is required because their hepatic characteristics, such as drug metabolism capacity, are lower than those of PHs [6].

To promote further maturation of the hepatocyte-like cells, we subjected them to three-dimensional (3D) spheroid cultures. It is known that various 3D culture conditions (such as Alginate scaffolds [7], cell sheet technology [8], galactose-carrying substrata [9], and basement membrane substratum [10]) are useful for the maturation of the hepatocyte-like cells. Nanopillar Plate technology [11] used in the present study makes it easy to control the configuration of the spheroids. The Nanopillar Plate has an arrayed  $\mu$ m-scale hole structure at the bottom of each well, and nanopillars were aligned further at the bottom of the respective holes. The seeded cells evenly drop into the holes, then migrate and aggregate on top surface of the nanopillars, thus likely to form the uniform spheroids in each hole. Not only 3D spheroid cultures [12] but also Matrigel overlay cultures [13] are useful for maintaining the hepatocyte characteristics of PHs. Therefore, we employed both 3D

\* Corresponding author. Laboratory of Biochemistry and Molecular Biology, Graduate School of Pharmaceutical Sciences, Osaka University, 1-6 Yamadaoka, Suita, Osaka 565-0871, Japan. Tel.: +81 6 6879 8185; fax: +81 6 6879 8186.

E-mail address: [mizuguch@phs.osaka-u.ac.jp](mailto:mizuguch@phs.osaka-u.ac.jp) (H. Mizuguchi).

spheroid culture and Matrigel overlay culture systems to promote hepatocyte maturation of the hepatocyte-like cells.

The hepatocyte-like cells generated from hESCs/hiPSCs are expected to be used in drug development. To the best of our knowledge, however, few studies have tried to predict widespread drug-induced cytotoxicity *in vitro* using the hepatocyte-like cells. To precisely determine the applicability of the hepatocyte-like cells to drug screening, it is necessary to investigate the responses of these hepatocyte-like cells to many kinds of hepatotoxic drugs.

In this study, 3D spheroid and Matrigel overlay cultures of the hepatocyte-like cells were performed to promote hepatocyte maturation. The gene expression analysis of cytochrome P450 (CYP) enzymes, conjugating enzymes, hepatic transporters, and hepatic nuclear receptors in the 3D spheroid-cultured hESC- or hiPSC-derived hepatocyte-like cells (3D ES-hepa or 3D iPSC-hepa), were analyzed. In addition, CYP induction potency and drug metabolism capacity were estimated in the 3D ES/iPSC-hepa. To determine the suitability of these cells for drug screening, we examined whether the drug-induced cytotoxicity is induced by treatment of various kinds of hepatotoxic drugs in 3D ES/iPSC-hepa.

## 2. Materials and methods

### 2.1. hESCs and hiPSCs culture

A hESC line, H1 and H9 (WiCell Research Institute), was maintained on a feeder layer of mitomycin C-treated mouse embryonic fibroblasts (Millipore) with Repro Stem medium (Repro CELL) supplemented with 5 ng/ml fibroblast growth factor 2 (FGF2) (Sigma). Both H1 and H9 were used following the Guidelines for Derivation and Utilization of Human Embryonic Stem Cells of the Ministry of Education, Culture, Sports, Science and Technology of Japan and furthermore, and the study was approved by Independent Ethics Committee.

Three human iPSC lines were provided from the JCRB Cell Bank (Tic, JCRB Number: JCRB1331; Dotcom, JCRB Number: JCRB1327; Toe, JCRB Number: JCRB1338) [14,15]. These human iPSC lines were maintained on a feeder layer of mitomycin C-treated mouse embryonic fibroblasts with iPSELLon (Cardio) supplemented with 10 ng/ml FGF2. Other three human iPSC lines, 201B6, 201B7 and 253G1 were kindly provided by Dr. S. Yamanaka (Kyoto University) [2]. These human iPSC lines were maintained on a feeder layer of mitomycin C-treated mouse embryonic fibroblasts with Repro Stem supplemented with 5 ng/ml FGF2.

### 2.2. *In vitro* differentiation

Before the initiation of cellular differentiation, the medium of hESCs was exchanged into a defined serum-free medium, hESF9, and cultured as previously reported [16]. The differentiation protocol for the induction of definitive endoderm cells, hepatoblasts, and hepatocytes was based on our previous reports with some modifications [3–5,17]. Briefly, in mesoderm differentiation, hESCs were dissociated into single cells by using Accutase (Millipore) and cultured for 2 days on Matrigel (BD Biosciences) in differentiation hESF-DIF medium which contains 100 ng/ml Activin A (R&D Systems) and 10 ng/ml bFGF (hESF-DIF medium was purchased from Cell Science & Technology Institute; differentiation hESF-DIF medium was supplemented with 10 µg/ml human recombinant insulin, 5 µg/ml human apotransferrin, 10 µM 2-mercaptoethanol, 10 µM ethanolamine, 10 µM sodium selenite, and 0.5 mg/ml bovine fatty acid free serum albumin [all from sigma]). To generate definitive endoderm cells, the mesoderm cells were transduced with 3000 vector particle (VP)/cell of Ad-FOXA2 for 1.5 h on day 2 and cultured until day 6 on Matrigel in differentiation hESF-DIF medium supplemented with 100 ng/ml Activin A and 10 ng/ml bFGF. For induction of hepatoblasts, the DE cells were transduced with each 1500 VP/cell of Ad-FOXA2 and Ad-HNF1α for 1.5 h on day 6 and cultured for 3 days on Matrigel in hepatocyte culture medium (HCM) (Lonza) supplemented with 30 ng/ml bone morphogenetic protein 4 (BMP4) (R&D Systems) and 20 ng/ml FGF4 (R&D Systems). In hepatic expansion, the hepatoblasts were transduced with each 1500 VP/cell of Ad-FOXA2 and Ad-HNF1α for 1.5 h on day 9 and cultured for 3 days on Matrigel in HCM supplemented with 10 ng/ml hepatocyte growth factor (HGF), 10 ng/ml FGF1, 10 ng/ml FGF4, and 10 ng/ml FGF10 (all from R&D Systems). To perform hepatocyte maturation on Nanopillar Plate (a prototype multi-well culturing plate for spheroid culture developed and prepared by Hitachi High-Technologies Corporation) shown in Fig. 1B, the cells were seeded at  $2.5 \times 10^5$  cells/cm<sup>2</sup> (Fig. S1) in hepatocyte culture medium (Fig. S2) supplemented with 10 ng/ml HGF, 10 ng/ml FGF1, 10 ng/ml FGF4, and 10 ng/ml FGF10 on day 11. In the first stage of hepatocyte maturation (from day 12 to day 25), the cells were cultured for 13 days on Matrigel in HCM supplemented with 20 ng/ml HGF,

20 ng/ml oncostatin M (OsM), 10 ng/ml FGF4, and  $10^{-6}$  M dexamethasone (DEX). In the second stage of hepatocyte maturation (from day 25 to day 35), Matrigel was overlaid on the hepatocyte-like cells. Matrigel were diluted to a final concentration of 0.25 mg/ml with William's E medium (Invitrogen) containing 4 mM L-glutamine, 50 µg/ml gentamycin sulfate,  $1 \times$  ITS (BD Biosciences), 20 ng/ml OsM, and  $10^{-6}$  M DEX. The culture medium was aspirated, and then the Matrigel solution (described above) was overlaid on the hepatocyte-like cells. The cells were incubated overnight, and the medium was replaced with HCM supplemented with 20 ng/ml OsM and  $10^{-6}$  M DEX.

### 2.3. Adenovirus (Ad) vectors

Ad vectors were constructed by an improved *in vitro* ligation method [18,19]. The human EF-1α promoter-driven LacZ-, FOXA2-, or HNF1α-expressing Ad vectors (Ad-LacZ, Ad-FOXA2, or Ad-HNF1α, respectively) were constructed previously [3,4,20]. All of Ad vectors contain a stretch of lysine residue (K7) peptides in the C-terminal region of the fiber knob for more efficient transduction of hESCs, hiPSCs, and DE cells, in which transfection efficiency was almost 100%, and purified as described previously [3–5]. The vector particle (VP) titer was determined by using a spectrophotometric method [21].

### 2.4. Flow cytometry

Single-cell suspensions of hESC/hiPSC-derived cells were fixed with 2% paraformaldehyde (PFA) at 4°C for 20 min, and then incubated with the primary antibody (described in Table S1), followed by the secondary antibody (described in Table S1). Flow cytometry analysis was performed using a FACS LSR Fortessa flow cytometer (BD Biosciences).

### 2.5. RNA isolation and reverse transcription-polymerase chain reaction (RT-PCR)

Total RNA was isolated from hESCs or hiPSCs and their derivatives using ISO-GENE (Nippon Gene). cDNA was synthesized using 500 ng of total RNA with a Superscript VILLO cDNA synthesis kit (Invitrogen). Real-time RT-PCR was performed with Taqman gene expression assays (Applied Biosystems) or SYBR Premix Ex Taq (TaKaRa) using an ABI PRISM 7000 Sequence Detector (Applied Biosystems). Relative quantification was performed against a standard curve and the values were normalized against the input determined for the housekeeping gene, glyceraldehyde 3-phosphate dehydrogenase (GAPDH). The primer sequences used in this study are described in Table S2.

### 2.6. Immunohistochemistry

The cells were fixed with 4% PFA. After incubation with 1% Triton X-100, blocking with Blocking One (Nakalai tesque), the cells were incubated with primary antibody (described in Table S1) at 4°C for overnight, followed by incubation with a secondary antibody (described in Table S1) at room temperature for 1 h.

### 2.7. ELISA

The hESCs or hiPSCs were differentiated into hepatocytes as described in Fig. 1A. The culture supernatants, which were incubated for 24 h after fresh medium was added, were collected and analyzed for the amount of ALB secretion by ELISA. ELISA kits for ALB were purchased from Bethyl. ELISA was performed according to the manufacturer's instructions. The amount of ALB secretion was calculated according to each standard followed by normalization to the protein content per well.

### 2.8. Urea secretion

The hESCs or hiPSCs were differentiated into hepatocytes as described in Fig. 1A. The culture supernatants, which were incubated for 24 h after fresh medium was added, were collected and analyzed for the amount of urea secretion. Urea measurement kits were purchased from BioAssay Systems. The experiment was performed according to the manufacturer's instructions. The amount of urea secretion was calculated according to each standard followed by normalization to the protein content per well.

### 2.9. Canalicular secretory assay

At cellular differentiation, the hepatocyte-like cell spheroids were treated with 5 mM choly-l-lysyl-fluorescein (CLF) (BD Biosciences) for 30 min. The cells were washed with culture medium, and then observed by fluorescence microscope. To inhibit the function of BSEP, the cells were pretreated with Cyclosporin A 24 h before of the CLF treatment.

### 2.10. Assay for CYP activity and CYP induction

To measure the cytochrome P450 2C9 and 3A4 activity of the cells, we performed lytic assays by using a P450-Glo™ CYP2C9 (catalog number; V8791) and



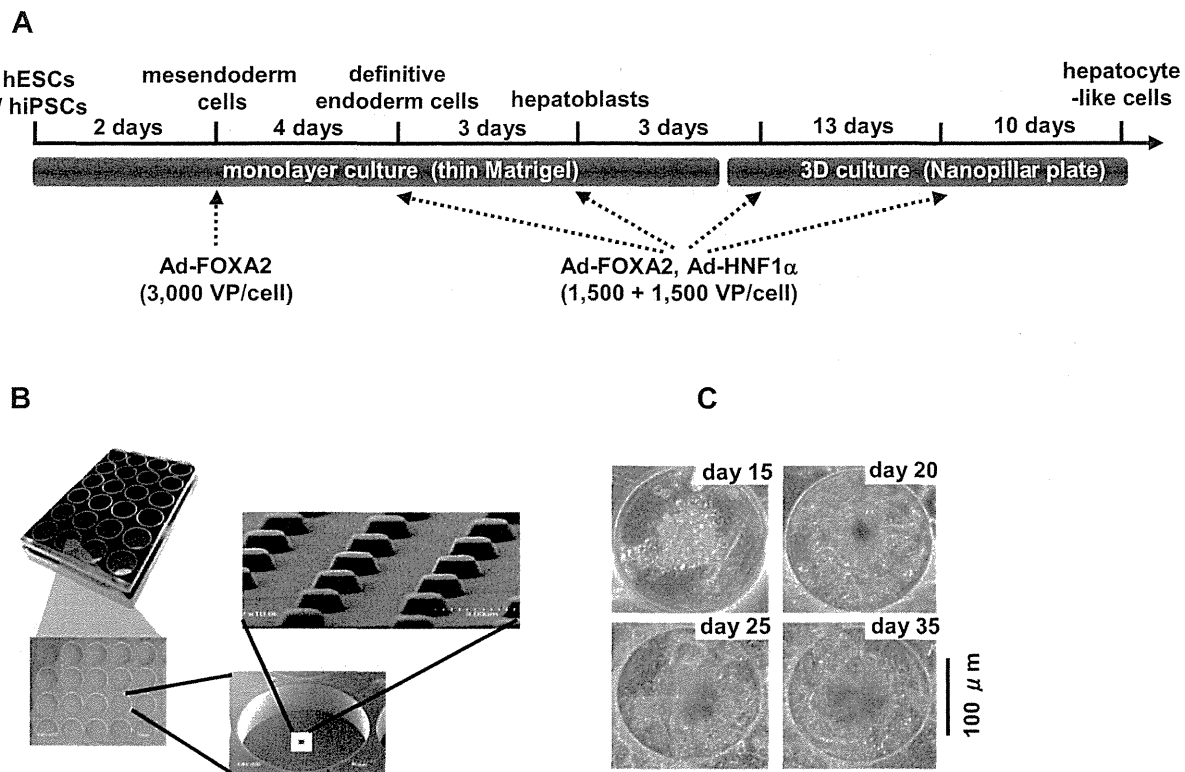


**Fig. 1.** Hepatocyte-like cells were differentiated from hESCs/hiPSCs by using Nanopillar Plate. (A) The procedure for differentiation of hESCs into 3D ES/iPS-hepa via mesendoderm cells, definitive endoderm cells, and hepatoblasts is presented schematically. In the differentiation, not only the addition of growth factors but also stage-specific transient transduction of both FOXA2- and HNF1 $\alpha$ -expressing Ad vector (Ad-FOXA2 and Ad-HNF1 $\alpha$ , respectively) was performed. The cellular differentiation procedure is described in detail in the materials and methods section. (B) Photograph display of a 24-well format Nanopillar Plate and its microstructural appearances of the hole and pillar structure. (C) Phase-contrast micrographs of the hESC-hepa spheroids on the Nanopillar Plate are shown. Scale bar represents 100  $\mu$ m.

3A4 (catalog number; V9001) Assay Kit (Promega), respectively. We measured the fluorescence activity with a luminometer (Lumat LB 9507; Berthold) according to the manufacturer's instructions. The CYP activity was normalized with the protein content per well.

To measure CYP2C9 and 3A4 induction potency, the CYP activity was measured by using a P450-GloTM CYP2C9 and 3A4 Assay Kit, respectively. The cells were treated with rifampicin, which is known to induce both CYP2C9 and 3A4, at a final concentration of 10  $\mu$ M for 48 h. The cells were also treated with Ketoconazole (Sigma) or Sulfaphenazole (Sigma), which are inhibitors for CYP3A4 or 2C9, at a final concentration of 1  $\mu$ M or 2  $\mu$ M, respectively, for 48 h. Controls were treated with DMSO (final concentration 0.1%). Inducer compounds were replaced daily.

#### 2.11. Cell viability tests

Cell viability was assessed by the WST-8 assay kit (Dojindo) in Fig. 2D. After treatment with test compounds, such as Acetaminophen (Wako), Allopurinol (Wako), Amiodaron (Sigma), Benzbromarone (Sigma), Clozapine (Wako), Cyclizine (MP bio), Dantrolene (Wako), Desipramine (Wako), Disulfiram (Wako), Erythromycin (Wako), Felbamate (Sigma), Flutamide (Wako), Isoniazid (Sigma), Labetalol (Sigma), Lefunomide (Sigma), Maprotiline (Sigma), Nefazodone (Sigma), Nitrofurantoin (Sigma), Sulindac (Wako), Tacrine (Sigma), Tebinafine (Wako), Tolcapone (TRC), Troglitazone (Wako), and Zafirlukast (Cayman) for 24 h, the cell viability was measured. The cell viability of the 3D iPS-hepa were assessed by WST-8 assay after 24 h exposure to different concentrations of Aflatoxin B1 (Sigma) and Benzbromarone in the presence or absence of the CYP3A4 or 2C9 inhibitor, Ketoconazole (1  $\mu$ M) or Sulfaphenazole (10  $\mu$ M), respectively. The control refers to incubations in the absence of test compounds and was considered as 100% viability value. Controls were treated with DMSO (final concentration 0.1%). ATP assay (BioAssay Systems), Alamar Blue assay (Invitrogen), and Crystal Violet (Wako) staining assay were performed according to the manufacturer's instructions.

#### 2.12. Primary human hepatocytes

Three lots of cryopreserved human hepatocytes (lot Hu8072 [CellDirect], HC2-14, and HC10-101 [Xenotech]) were used. These three lots of cryopreserved human hepatocytes were cultured according to our previous report [5].

#### 2.13. Statistical analysis

Statistical analysis was performed using the unpaired two-tailed Student's *t*-test. All data are represented as means  $\pm$  SD ( $n = 3$ ).

### 3. Results

The 3D ES/iPS-hepa were generated from hESCs/hiPSCs as shown in Fig. 1A. Hepatocyte differentiation of hESCs/hiPSCs was efficiently promoted by stage-specific transient transduction of FOXA2 and HNF1 $\alpha$  in addition to the treatment with appropriate soluble factors (growth factors and cytokines) [6]. On day 11, the hESC-derived cells were seeded at  $2.5 \times 10^5$  cells/cm<sup>2</sup> (Fig. S1) on Nanopillar Plate (Fig. 1B), in hepatocyte culture medium (Fig. S2) to promote hepatocyte maturation. In addition, Matrigel was overlaid on the 3D ES-hepa to promote further hepatocyte maturation. The 3D ES-hepa with compact morphology that were adhesive to the substratum and had an optimal size (approximately 100  $\mu$ m in diameter) were formed by using the Nanopillar Plate (Fig. 1C). The spheroids seem to be stable because they could be cultured for more than 20 days. We have confirmed that more than 90% of the cells that constitute the spheroids were alive, indicating that the necrotic centers are absent.

To investigate whether or not a 3D spheroid culture could promote hepatocyte maturation of the hepatocyte-like cells, various hepatocyte characteristics of the 3D ES/iPS-hepa were compared with those of the monolayer-cultured hESC- or hiPSC-derived hepatocyte-like cells (mono ES-hepa or mono iPS-hepa). The gene expression level of *ALB* peaked on day 20 in the mono ES-hepa, and then it was dramatically decreased after day 25 (Fig. 2A). In contrast, the gene expression level of *ALB* was



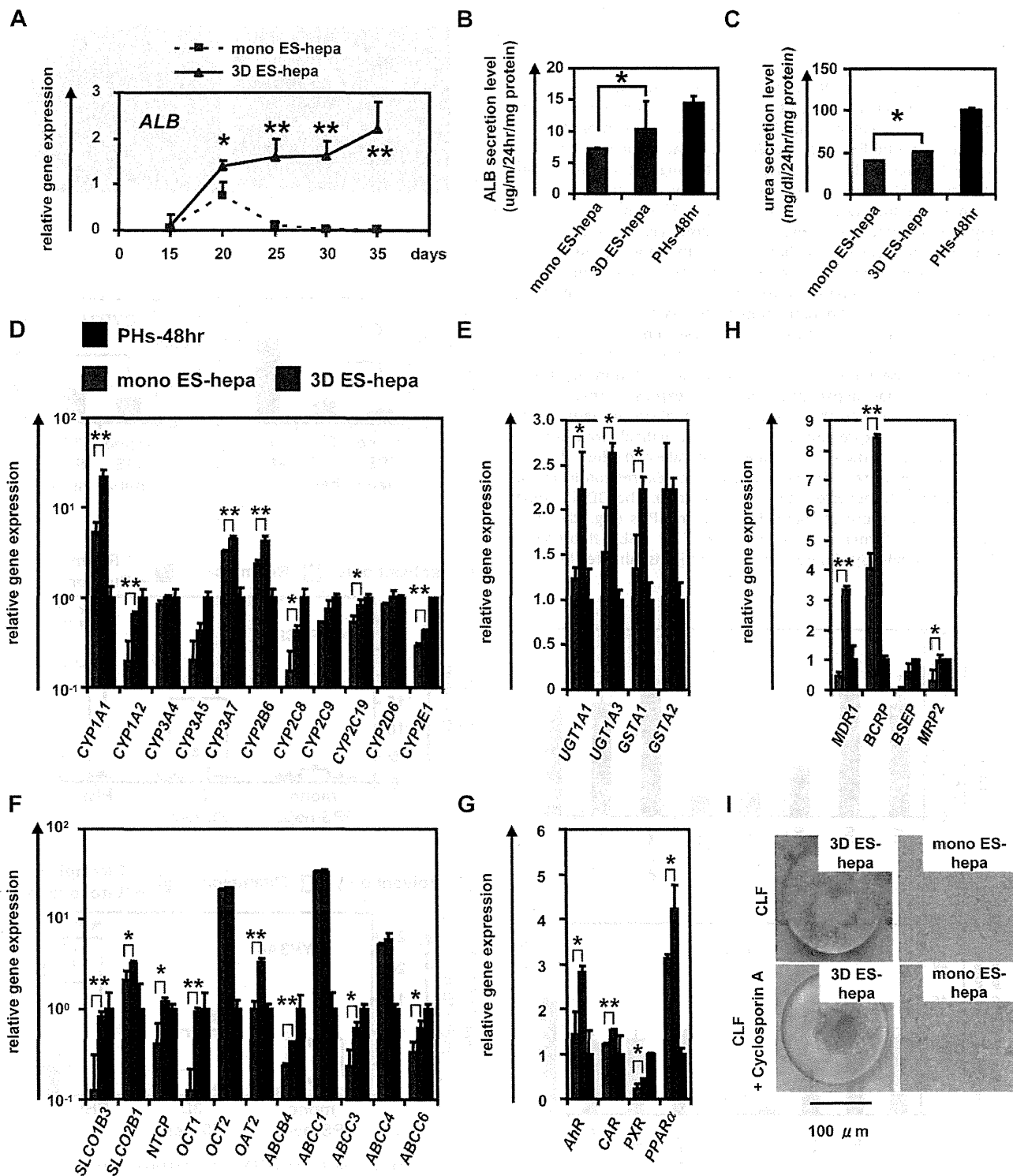


**Fig. 2.** Hepatocyte functions in hESC-derived hepatocyte-like cells were enhanced by using Nanopillar Plate. (A) The gene expression levels of *ALB* were measured by real-time RT-PCR on day 15, 20, 25, 30, and 35. On the y axis, the gene expression levels in PHs (three lots of PHs were used in all studies), which were cultured for 48 h after plating (PHs-48hr), were taken as 1.0. (B, C) The amount of ALB (B) and urea (C) secretion were examined in the mono ES-hepa (day 20), the 3D ES-hepa (day 35), and PHs-48hr. (D–H) The gene expression levels of CYP enzymes (D), conjugating enzymes (E), hepatic transporters (F), hepatic nuclear receptors (G), and bile canalicular transporters (H) were examined by real-time RT-PCR in the mono ES-hepa, the 3D ES-hepa, and PHs-48hr. On the y axis, the expression levels in PHs-48hr were taken as 1.0. (I) The ability of bile acid uptake and efflux was examined in the mono ES-hepa and 3D ES-hepa. Choly-l-tyrosyl-fluorescein (CLF) (5  $\mu$ M) was used for the observation of bile canalicular uptake and efflux. To inhibit transportation by BSEP, the cells were pretreated with 1  $\mu$ M Cyclosporin A. \**P* < 0.05; \*\**P* < 0.01.

moderately increased in the 3D ES-hepa until day 35 (Fig. 2A). These results suggest that the hepatocyte functions of the 3D ES-hepa are sustained for more than 2 weeks on the Nanopillar Plate, although those of the mono ES-hepa are rapidly devitalized (Fig. 2A and Fig. S4). Other hepatocyte characteristics, such as ability of ALB and urea secretion and gene expression levels of hepatocyte-related markers in the 3D ES-hepa were compared with those of the mono ES-hepa (Fig. 2B–H). Because the gene expression level of *ALB* in the 3D ES-hepa was the highest on day 35 and that in mono ES-hepa was the highest on day 20, various hepatocyte characteristics were compared on day 35 or day 20, respectively. The amount of ALB (Fig. 2B) and urea (Fig. 2C) secretion in the 3D ES-hepa was higher than those of the mono ES-hepa. The gene expression levels of CYP enzymes (Fig. 2D), conjugating enzymes (Fig. 2E), hepatic transporters (Fig. 2F), hepatic nuclear receptors (Fig. 2G), and hepatic transcription factors (Fig. S5) in the 3D ES-hepa were higher than those in the mono ES-hepa. The expression levels of most of the genes in the 3D ES-hepa were higher than those in the mono ES-hepa. Because the previous study [11] showed that hepatocyte spheroids expressed hepatocyte transporters similar to those of the bile canaliculi in native liver tissue, the gene expression levels of bile canaliculi transporters (Fig. 2H), as well as the ability of bile acid uptake and efflux, (Fig. 2I) were examined in the 3D ES-hepa. The gene expression levels of bile canaliculi transporters were increased in the 3D ES-hepa compared with those of mono ES-hepa and PHs (Fig. 2H). The bile canaliculi formation was visualized by BSEP fluorescent substrate: Cholyl-L-tyrosyl-fluorescein (CLF), which is inhibited by BSEP

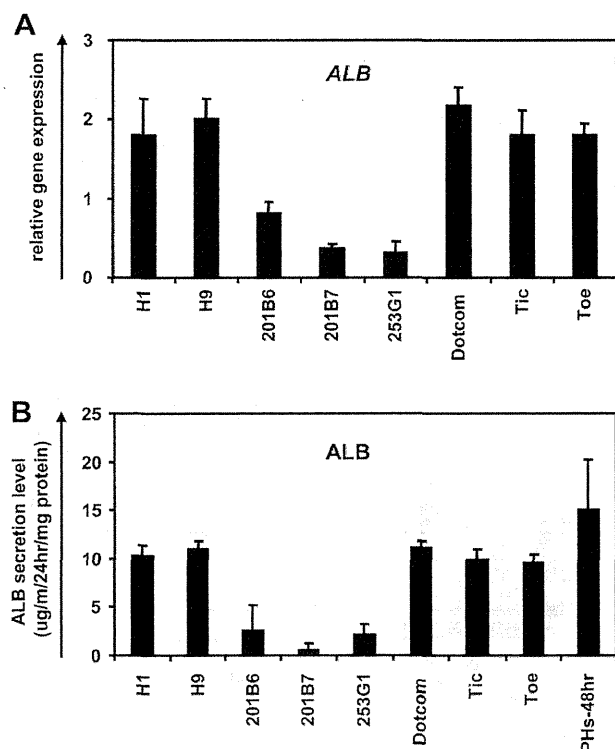


**Fig. 3.** Comparison of the hepatic differentiation capacities of various hESC and hiPSC lines hESCs (H1 and H9) and hiPSCs (201B6, 201B7, 253G1, Dotcom, Tic, and Toe) were differentiated into the 3D ES/iPS-hepa as described in Fig. 1A. (A) On day 20, the gene expression level of *ALB* was examined by real-time RT-PCR. On the y axis, the gene expression level of *ALB* in PHs-48hr was taken as 1.0. (B) On day 20, the amount of ALB secretion was examined by ELISA. The amount of ALB secretion was calculated according to each standard followed by normalization to the protein content per well.

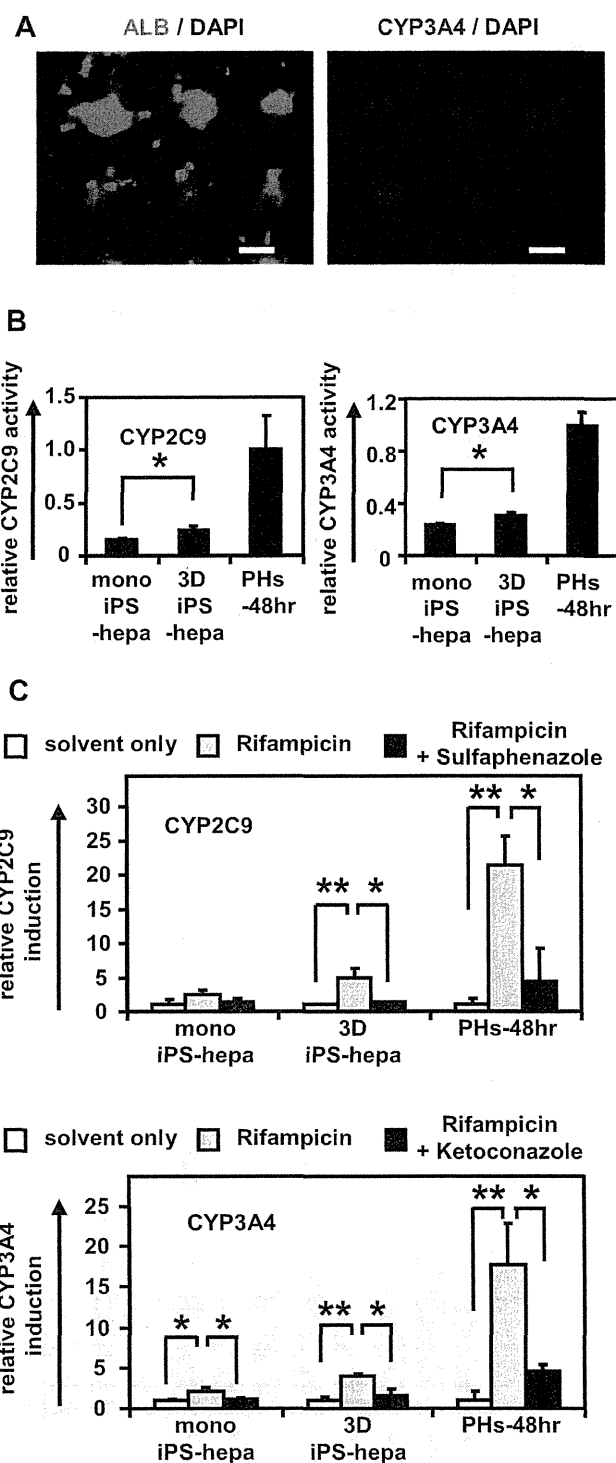
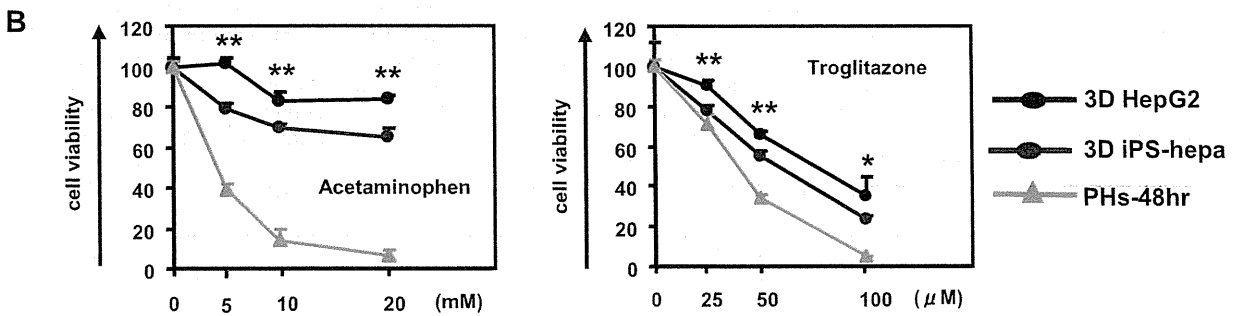
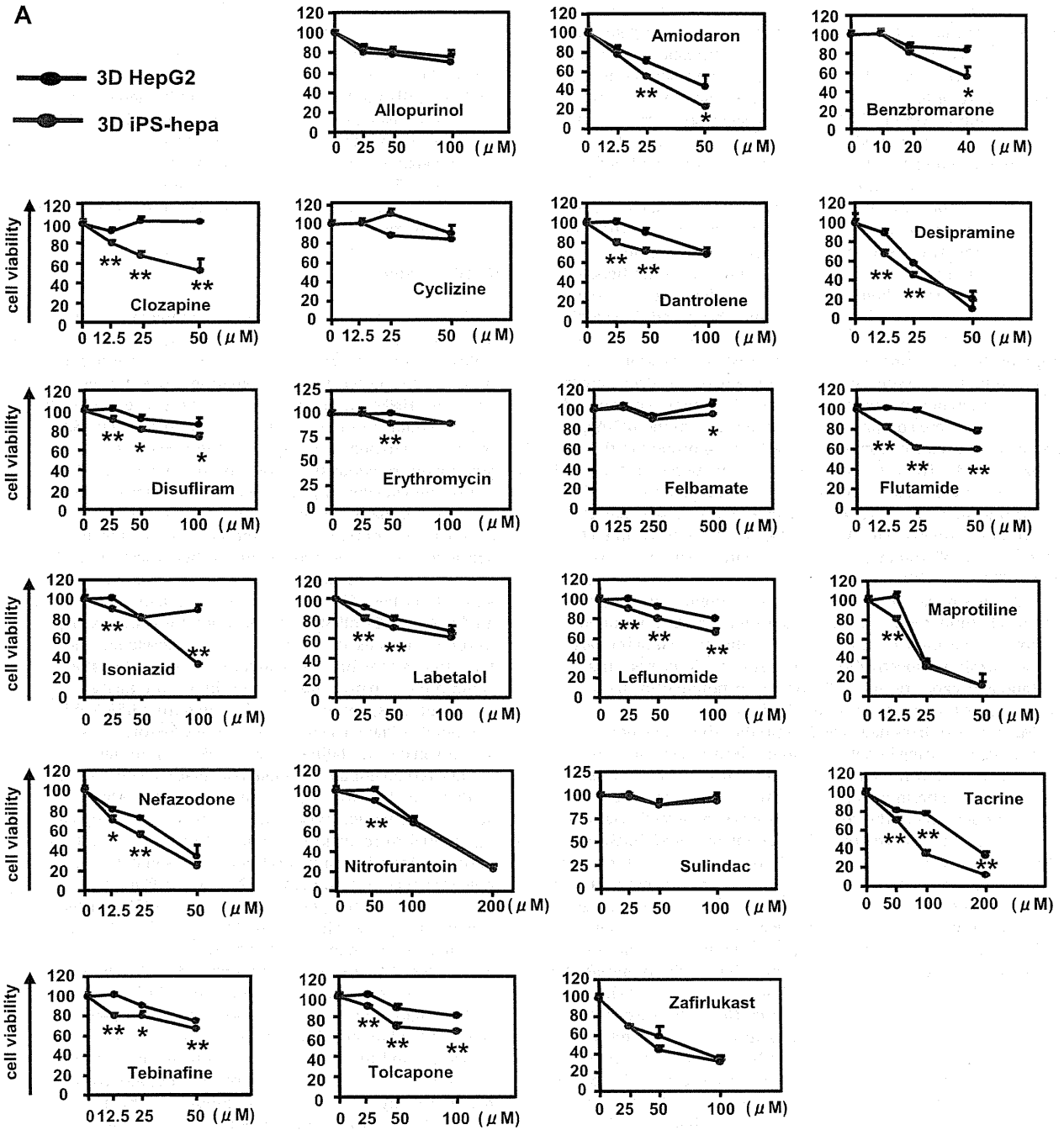


**Fig. 4.** Drug metabolism capacity and CYP induction potency were examined in the 3D iPS-hepa. (A) The 3D iPS-hepa (day 35) were subjected to immunostaining with anti-ALB (green) or CYP3A4 (red) antibodies. Nuclei were counterstained with DAPI (blue). Scale bar represents 100  $\mu$ m. (B) The CYP activity was measured in the mono iPS-hepa (day 20), the 3D iPS-hepa (day 35), and PHs-48hr. On the y axis, the CYP activity in PHs-48hr was taken as 1.0. (C) Induction of CYP2C9 (left) or CYP3A4 (right) by DMSO (solvent only; white bar), Rifampicin (gray bar), or rifampicin and CYP inhibitor (Sulfafanazole or Ketoconazole, black bar) in the mono iPS-hepa, the 3D iPS-hepa, and PHs-48hr. On the y axis, the CYP activity of the cells that have been cultured in DMSO-containing medium was taken as 1.0. \* $P < 0.05$ ; \*\* $P < 0.01$ .



inhibitor Cyclosporin A [22,23]. More CLF was accumulated in the 3D ES-hepa than in the mono ES-hepa (Fig. 2I upper panel). Moreover, CLF accumulation was inhibited by Cyclosporin A treatment only in the 3D ES-hepa (Fig. 2I lower panel), demonstrating that the functionality of BSEP transporter in 3D ES-hepa was greater than that in mono ES-hepa. These results suggested that hepatocyte maturation was promoted by the culture on the Nanopillar Plate. It is likely that, compared to the monolayer culture condition, the 3D spheroid-culture condition is more similar to the *in vivo* condition.

It is important to select an hESC/hiPSC line that has a strong ability to differentiate into hepatocyte-like cells in the case of medical applications such as drug screening. In this study, two hESC lines and six hiPSC lines were differentiated into the hepatocyte-like cells, and then their gene expression levels of *ALB* (Fig. 3A) and *ALB* secretion levels (Fig. 3B) were compared. These results suggest that the iPSC line, Dotcom, was the suitable cell line for hepatocyte maturation. Therefore, the iPSC line, Dotcom, was used to examine the possibility of the 3D iPSC-hepa for drug screening. The drug metabolism capacity and the CYP induction potency of the 3D iPSC-hepa were compared with those of the mono iPSC-hepa. We confirmed the expression of *ALB* and CYP3A4 protein in the 3D ES-hepa (Fig. 4A). The activity levels of CYP enzymes in the 3D iPSC-hepa were measured according to the metabolism of the CYP2C9 or CYP3A4 substrates (Fig. 4B); the levels were higher than those of the mono iPSC-hepa (Fig. 4B). We further tested the induction of CYP2C9 and CYP3A4 by chemical stimulation (rifampicin was used as a CYP2C9 or CYP3A4 inducer). Compared with mono iPSC-hepa, the 3D iPSC-hepa produced more metabolites in response to chemical stimulation (Fig. 4C). In addition, the CYP induction was inhibited by using CYP2C9 or CYP3A4 inhibitor (Sulfaphenazole or Ketoconazole, respectively). These results indicated that drug metabolism capacity and CYP induction potency in 3D iPSC-hepa were higher than those in mono iPSC-hepa.

Many researchers have tried to predict the drug-induced cytotoxicity *in vitro* using hepatocarcinoma-derived cells such as HepG2 cells [24,25]. HepG2 cells are less expensive than PHs and the reproducible experiments are easier to perform than they are with PHs, although 30% of the compounds were incorrectly classified as nontoxic [24,25]. To overcome these problems, hESC/hiPSC-derived hepatocyte-like cells are expected to be used to predict drug-induced cytotoxicity. To examine its applicability to drug screening, the 3D iPSC-hepa were treated with various drugs, that cause hepatotoxicity. WST-8 assay was performed to evaluate cell viability (Fig. S6). The susceptibility of the 3D iPSC-hepa to most of the hepatotoxic drugs was higher than that of the mono iPSC-hepa (Fig. S7). Compared to the mono iPSC-hepa, the 3D iPSC-hepa were more suitable tools for drug screening. Next, the susceptibility of the 3D iPSC-hepa to the hepatotoxic drugs was compared with that of the 3D spheroid cultured HepG2 cells (3D HepG2; the hepatocyte functions of 3D HepG2 cells are higher than those of monolayer cultured HepG2 cells [Fig. S8]). With most of the drugs, the cell viability of the 3D iPSC-hepa was lower than that of the 3D HepG2 (Fig. 5A). These results indicated that the 3D iPSC-hepa are more valuable tools for drug screening than the 3D HepG2. However, the susceptibility of the 3D iPSC-hepa to Acetaminophen and Troglitazone was lower than that of the PHs which were cultured for 48 h after the cells were plated (Fig. 5B). These results might be due to the lower activity levels of CYPs in 3D iPSC-hepa as compared as those in PHs. Taken together, 3D iPSC-hepa are more valuable tools for drug screening than the 3D HepG2, although further maturation

of 3D iPSC-hepa is still required for 3D iPSC-hepa to be an alternative cell source of PHs in the drug screening.

To examine whether drug-induced cytotoxicity is caused by CYP metabolites in 3D iPSC-hepa, Aflatoxin B1 (mainly metabolized by CYP3A4 [26]) and Benzbromarone (mainly metabolized by CYP2C9 [27]) were treated in the presence or absence of a CYP3A4 and a 2C9 inhibitor, Ketoconazole and Sulfaphenazole, respectively (Fig. 6). The cell viability of 3D iPSC-hepa was partially rescued by treatment with the CYP inhibitor. These results indicated that drug-induced cytotoxicity was caused by CYP metabolites of Aflatoxin B1 and Benzbromarone.

#### 4. Discussion

Recently, it has been expected that human pluripotent stem cells and their derivatives, including hepatocyte-like cells, will be utilized in applications for the safety assessment of drugs. We have previously reported that combinational overexpression of SOX17, HEX, and HNF4 $\alpha$ , or combinational overexpression of FOXA2 and HNF1 $\alpha$  could promote hepatocyte differentiation [5,6]. However, the drug metabolism capacity of the hepatocyte-like cells generated by our previous protocol was still lower than that of primary human hepatocytes [6]. To generate more matured hepatocyte-like cells as compared with our previous protocol, we established a hepatocyte differentiation method employing not only stage-specific transient overexpression of hepatocyte-related transcription factors but also a 3D culture systems using a Nanopillar Plate, was established. Although the use of hepatocyte-like cells generated from hESCs/hiPSCs in application for drug toxicity testing has begun to be focused, to the best of our knowledge, there have been few studies that have investigated whether hepatocyte-like cells could predict many kinds of drug-induced toxicity.

3D culture spheroids were generated from hESCs/hiPSCs by using a Nanopillar Plate. The diameter of the spheroids was approximately 100  $\mu$ m on day 35 of differentiation (Fig. 1C). Because it is known that the no-oxygen limitation would take place in spheroids up to 100  $\mu$ m in diameter [28], the size of the spheroid might be important to generate spheroids with high viability. A Nanopillar Plate has a potential to regulate the spheroid diameter simply by culturing under optimized seeding condition, on its suitably designed pillar and hole structure [11]. Therefore, a Nanopillar Plate would be a suitable environment for the generation of 3D ES/iPSC-hepa that show high viability and possess high level of hepatocellular functions.

The levels of many hepatocyte functions, such as *ALB* secretion ability (Fig. 2B), urea secretion ability (Fig. 2C), hepatocyte-related gene expressions (Fig. 2D–H), drug metabolism capacity (Fig. 4B), and CYP induction potency (Fig. 4C), of 3D ES/iPSC-hepa were higher than those of mono ES/iPSC-hepa. This might have been because the structural and functional polarity, which can be seen in the naïve environment of hepatocytes, of the hepatocyte-like cells was configured by a 3D culturing condition. Previous studies have shown that a 3D culture condition is suitable to maintain the hepatic characteristics of the isolated hepatocytes because this condition mimic *in vivo* environment [29,30]. These facts indicated that the 3D culture condition is a more suitable condition for the hepatocyte-like cells than the monolayer culture condition.

Two hES cell lines and six hiPS cell lines were differentiated into the hepatocyte-like cells in this study. The hiPS cell line, Dotcom, seemed to be a suitable cell line for hepatic differentiation (Fig. 3). Because the hepatic differentiation propensity differs among the

**Fig. 5.** The possibility of applying 3D iPSC-hepa to drug testing was examined. (A) The cell viability of the 3D HepG2 (black) and 3D iPSC-hepa (red) were assessed by WST-8 assay after 24 h exposure to different concentrations of 22 test compounds. (B) The cell viability of the 3D HepG2 (black), 3D iPSC-hepa (red), and PHs-48hr (green) were assessed by WST-8 assay after 24 h exposure to different concentrations of Acetaminophen and Troglitazone. Cell viability is expressed as a percentage of cells treated with solvent only. \* $P < 0.05$ ; \*\* $P < 0.01$ .